

Anharmonicity, mechanical instability, and thermodynamic properties of the Cr-Re - phase

Mauro Palumbo, Suzana G. Fries, Alain Pasturel, and Dario Alfè

Citation: *The Journal of Chemical Physics* **140**, 144502 (2014); doi: 10.1063/1.4869800

View online: <http://dx.doi.org/10.1063/1.4869800>

View Table of Contents: <http://scitation.aip.org/content/aip/journal/jcp/140/14?ver=pdfcov>

Published by the [AIP Publishing](#)

Articles you may be interested in

Elastic, superconducting, and thermodynamic properties of the cubic metallic phase of AlH₃ via first-principles calculations

J. Appl. Phys. **114**, 114905 (2013); 10.1063/1.4821287

Pressure induced structural phase transition in solid oxidizer KClO₃: A first-principles study

J. Chem. Phys. **138**, 174701 (2013); 10.1063/1.4802722

Ab-initio approach to the electronic, structural, elastic, and finite-temperature thermodynamic properties of Ti₂AX (A=Al or Ga and X=C or N)

J. Appl. Phys. **110**, 093504 (2011); 10.1063/1.3652768

Segregation of tungsten at (L1₂) / (fcc) interfaces in a Ni-based superalloy: An atom-probe tomographic and first-principles study

Appl. Phys. Lett. **93**, 201905 (2008); 10.1063/1.3026745

Spin-glass-like static and dynamic properties of mechanically alloyed Fe-Re-Cr

J. Appl. Phys. **87**, 6534 (2000); 10.1063/1.372761



Re-register for Table of Content Alerts

Create a profile.



Sign up today!



Anharmonicity, mechanical instability, and thermodynamic properties of the Cr-Re σ -phase

Mauro Palumbo,^{1,a)} Suzana G. Fries,¹ Alain Pasturel,² and Dario Alfè³

¹ICAMS, Ruhr University Bochum, Universität Str. 150, D-44801 Bochum, Germany

²SIMAP, UMR CNRS-INPG-UJF 5266, BP 75, F-38402 Saint Martin d'Hères, France

³Department of Earth Sciences, Department of Physics and Astronomy, London Centre for Nanotechnology and Thomas Young Centre@UCL, University College London, Gower Street, London WC1E 6BT, United Kingdom

(Received 21 October 2013; accepted 18 March 2014; published online 8 April 2014)

Using density-functional theory in combination with the direct force method and molecular dynamics we investigate the vibrational properties of a binary Cr-Re σ -phase. In the harmonic approximation, we have computed phonon dispersion curves and density of states, evidencing structural and chemical effects. We found that the σ -phase is mechanically unstable in some configurations, for example, when all crystallographic sites are occupied by Re atoms. By using a molecular-dynamics-based method, we have analysed the anharmonicity in the system and found negligible effects (~ 0.5 kJ/mol) on the Helmholtz energy of the binary Cr-Re σ -phase up to 2000 K ($\sim 0.8T_m$). Finally, we show that the vibrational contribution has significant consequences on the disordering of the σ -phase at high temperature. © 2014 AIP Publishing LLC. [<http://dx.doi.org/10.1063/1.4869800>]

I. INTRODUCTION

Control of the formation of topologically close-packed (TCP) phases in steels and Ni-based superalloys is important specially for their high-temperature applications.¹ In order to achieve an enhancement of the mechanical properties, the precipitation process must occur under controlled conditions and to this end it is important to understand the thermodynamics of these phases, which in many cases are found stable only above room temperature. Furthermore, one of the TCP phases, the σ -phase, has often been assumed as a crystalline model for icosahedral local order glasses (IC glasses)² and is one of the closest crystalline approximant to dodecagonal quasicrystals.³ This intermetallic compound has a tetragonal unit cell (type $D8_b$, space group $P4_2/mnm$) with 30 atoms distributed over five different sites. The main features of some TCP phases have recently been reviewed.^{4,5} They have been extensively studied using first-principles methods such as density-functional theory (DFT) calculations,^{6–18} but mostly at 0 K. Vibrational properties have been calculated in the harmonic approximation in some Laves phases.^{19,20} Dubiel *et al.*¹⁵ have recently used first-principles to investigate the harmonic vibrational properties of two ordered configurations in the α - and σ -phases. In another work, the vibrational properties of a one-component σ -phase were investigated by molecular dynamics using an empirical pair interatomic potential.²¹ However, no attempt to compute anharmonic effects using first-principles methods in TCP phases has been reported till now.

In our previous works,^{13,16,22} we have computed thermodynamic properties and phase diagrams as a function of temperature and composition in binary and ternary systems using a generalized Bragg-Williams-Gorsky approximation. The computed results were satisfactory from a qualitative

point of view, but differ from experimental data to some extent. A possible reason for the remaining discrepancy between calculations and experiments is that vibrational properties were completely neglected in our previous studies. The importance of vibrational contributions, and in particular of anharmonic effects, on phase stability is still under debate and can be very different from one system to another.^{23–25}

For this reason, in the present work we have computed the vibrational properties of the binary Cr-Re σ -phase, first in the harmonic approximation and then including anharmonic effects. In the experimental Cr-Re phase diagram, the σ -phase is stable only above 500 K²⁶ and the vibrational Helmholtz energy may contribute to its high-temperature stabilization. Among all possible binary configurations obtained from permutations of the constituent atoms in the σ -structure, we focus our attention on the CrReCrReRe, which corresponds to the ideal composition.⁴ We refer with this notation to the different occupation of Cr and Re in the five Wyckoff positions (2a,4f,8i₁,8i₂,8j) of the σ -phase, i.e., Cr in 2a, Re in 4f, Cr in 8i₁, Re in 8i₂, Re in 8j. The corresponding composition is $X(\text{Re}) = 0.66$. According to DFT results at 0 K,¹⁶ this configuration is the most stable for the binary Cr-Re σ -phase. We also briefly discuss the pure Cr (CrCrCrCrCr) and Re (ReReReReRe) configurations, i.e., with all atomic sites in the σ -structure occupied by Cr and Re atoms, respectively. Finally, we present the thermodynamic properties of all binary configurations obtained in the harmonic approximation and discuss their relevance for high-temperature disorder in the σ -phase.

II. THE σ -PHASE

The σ -phase ($D8_b$) is an intermetallic phase of the group of Frank-Kasper phases,^{27,28} also known as TCP phases. The first coordination shells of the constituent atoms in these structures are formed by slightly distorted tetrahe-

^{a)}mauro.palumbo@rub.de

TABLE I. Crystal structure of the σ -phase: sites, Wyckoff symbols, atomic positions (average values) in the $P4_2/mmm$ (no. 136) space group, and coordination number (adapted from Ref. 4).

| Sublattice | Wyckoff | x | y | z | CN |
|------------|---------|----------------|----------------|----------------|----|
| 1 | $2a$ | 0 | 0 | 0 | 12 |
| 2 | $4f$ | $\simeq 0.399$ | x | 0 | 15 |
| 3 | $8i_1$ | $\simeq 0.464$ | $\simeq 0.131$ | 0 | 14 |
| 4 | $8i_2$ | $\simeq 0.741$ | $\simeq 0.066$ | 0 | 12 |
| 5 | $8j$ | $\simeq 0.187$ | x | $\simeq 0.251$ | 14 |

dra (Frank-Kasper polyhedra) with coordination numbers $Z = 12, 14, 15, 16$. Recently, an extended review on the σ -phase has been published.⁴ The crystal structure is tetragonal, described by the $P4_2/mmm$ space group (Table I), with five non-equivalent positions ($2a, 4f, 8i_1, 8i_2, 8j$), which present coordination numbers 12, 15, 14, 12, and 14, respectively (Fig. 1 and Table I). These five non-equivalent sites generate $2^5 = 32$ ordered configurations in a binary system and $3^5 = 243$ configurations in a ternary system. Since the Wyckoff sites $8i_1, 8i_2$, and $8j$ have the same multiplicity (8), several configurations yield the same composition by atom permutation. Thus, the 32 (243) configurations in a binary (ternary) system, give rise to 16 (90) distinct compositions.

III. METHODOLOGY

A. Harmonic phonon calculations using the direct (supercell) method

First-principles calculations were performed using density-functional theory (DFT) as implemented in the Vienna *Ab initio* Simulation Package (VASP) with plane wave basis sets.^{29–31} The calculations employed the generalized gradient approximation (GGA-PW91) of Perdew and Wang,³² the valence electrons were explicitly represented with projector augmented wave (PAW) pseudopotentials, and the k-point meshes were created using the Monkhorst-Pack scheme.³³ The standard pseudopotentials provided within the VASP package were used for Cr and Re (6 or 7 valence electrons). The plane wave cut-off energy was set to 450 eV in all calculations. The ground state (0 K) structure was determined by minimizing the Hellmann-Feynman forces using the

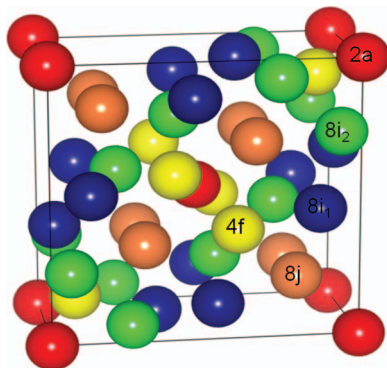


FIG. 1. Crystal structure of σ -phase.

conjugate gradient algorithm. Several relaxation steps were performed, both for internal atomic coordinates and lattice parameters, but keeping the cell symmetry. The k-point mesh in the last relaxation step was $8 \times 8 \times 15$ and both lattice parameters and internal atomic coordinates were allowed to relax. In comparison to our previous work,¹⁶ lower residual forces ($< 10^{-4}$ eV/Å) were obtained by relaxation, as necessary for the subsequent phonon calculations.

For phonon calculations in the harmonic approximation, we used the PHON package v. 1.35.³⁴ The dynamical matrix was obtained by the direct method (supercell method). For each relaxed σ -phase configuration, 12 atomic displacements were generated according to the crystal symmetry and atomic forces were computed using VASP. For the pure Re configuration (ReReReReRe), we further reduced numerical noise by employing central differences (24 atomic displacements). We tested different supercell sizes ($1 \times 1 \times 1, 1 \times 1 \times 2, 2 \times 2 \times 2$, and $2 \times 2 \times 3$) and found that the $1 \times 1 \times 2$ supercell provides results for the Helmholtz energy which converged within 0.2 kJ/mol at 2000 K. Similar tests were carried out to achieve the same precision target for the k-point mesh and we found the optimum being a $6 \times 6 \times 6$ k-point mesh for the $1 \times 1 \times 2$ supercell. The phonon DOS for each configuration was calculated by integrating over the first Brillouin zone with a equispaced q-points mesh of adequate size ($32 \times 32 \times 32$). Finally, the Helmholtz energy was calculated using the equation

$$F_{\text{harm}}(T) = \frac{1}{2} \sum_{\vec{q}, \nu} \hbar \omega(\vec{q}, \nu) + k_B T \sum_{\vec{q}, \nu} \ln \left(1 - e^{-\frac{\hbar \omega(\vec{q}, \nu)}{k_B T}} \right), \quad (1)$$

where $\omega(\vec{q}, \nu)$ are the phonon frequencies of mode ν and wavevector \vec{q} . The first term in the above equation is the Zero Point Energy (ZPE) and the second term is the phonon contribution at finite temperature. The sums in Eq. (1) are taken over the phonon modes ν and over all vectors \vec{q} in the Brillouin zone.

B. Anharmonicity using *ab initio* molecular dynamics and thermodynamic integration

In order to compute anharmonic effects, we employed *Ab Initio* Molecular Dynamics (AIMD) and Thermodynamic Integration (TI). We first used AIMD simulations to reveal changes in phonon frequencies at high temperatures. These simulations were performed within the framework of plane-wave-based DFT as implemented in the VASP package. We employed the same energy cutoff (450 eV), pseudopotentials and exchange-correlation functional (GGA-PW91) as in harmonic calculations (cf. Sec. III A). All the dynamical simulations were carried out in the NVT ensemble with a Nosé thermostat to control the temperature. Newton's equations of motion were integrated using Verlet's algorithm in the velocity form with a time step of 1 fs. Simulations were speeded up by a factor of two using an efficient extrapolation scheme for the charge density.³⁵ A $2 \times 2 \times 2$ supercell containing 240 atoms with periodic boundary conditions was used in the simulation. Only the Γ -point was considered to sample the supercell Brillouin zone. The phonon DOS was then obtained

by Fourier transform of the normalized velocity autocorrelation function.^{36,37}

To obtain a quantitative evaluation of the anharmonic Helmholtz energy, we used TI. This is a general technique to determine the difference in Helmholtz energies $F_1 - F_0$ between two systems whose total energies are U_1 and U_0 , respectively. $F_1 - F_2$ represents the reversible work done by switching (continuously and isothermally) the energy function from U_0 to U_1 . To this aim, a continuous variable energy function U_λ is introduced as

$$U_\lambda = (1 - \lambda)U_0 + \lambda U_1, \quad (2)$$

where the energy goes from U_0 to U_1 as λ goes from 0 to 1. In classical statistical mechanics, the work done in an infinitesimal change $d\lambda$ is

$$dF = \langle dU_\lambda/d\lambda \rangle_\lambda d\lambda, \quad (3)$$

where $\langle dU_\lambda/d\lambda \rangle_\lambda$ represents the thermal average for the system governed by U_λ . Then

$$F_1 - F_0 = \int_0^1 d\lambda \langle U_1 - U_0 \rangle_\lambda. \quad (4)$$

From a practical viewpoint, this last equation can be applied by calculating $d\lambda \langle U_1 - U_0 \rangle_\lambda$ for a suitable set of λ values and then performing the integration numerically. The average $d\lambda \langle U_1 - U_0 \rangle_\lambda$ needs to be evaluated by sampling over configurational space, usually by molecular dynamics. More details of the method can be found in Alfè *et al.*³⁸

In the present work, we used TI for computing $F_{\text{vib}} - F_{\text{harm}}$, where F_{vib} is the Helmholtz energy including anharmonic effects and F_{harm} is the Helmholtz energy in the harmonic approximation. To increase convergence speed we further introduced an intermediate reference system, whose energy and Helmholtz energy are U_{ref} and F_{ref} , and then applied twice thermodynamic integration by evaluating $F_{\text{vib}} - F_{\text{ref}}$ and $F_{\text{ref}} - F_{\text{harm}}$. Our intermediate reference system U_{ref} was the *ab initio* system sampled with a $2 \times 2 \times 2$ grid of k-points. We performed AIMD simulations at 9 values of

λ , each simulation lasting 15 ps. The canonical ensemble was simulated using the Andersen thermostat. The final step $F_{\text{vib}} - F_{\text{ref}}$ was performed using a perturbative approach to TI, in which we generated a set of statistical independent configurations using U_{ref} , and then computed

$$F_{\text{vib}} - F_{\text{ref}} = \langle U_{\text{vib}} - U_{\text{ref}} \rangle_{\text{ref}} - 1/2k_B T \langle \delta U^2 \rangle_{\text{ref}}, \quad (5)$$

where U_{vib} is the *ab initio* system sampled with a $6 \times 6 \times 6$ grid of k-points, $\delta U = U_{\text{vib}} - U_{\text{ref}} - \langle U_{\text{vib}} - U_{\text{ref}} \rangle_{\text{ref}}$, and $\langle U_{\text{vib}} - U_{\text{ref}} \rangle_{\text{ref}}$ represents the canonical average in the ensemble generated by U_{ref} . The perturbative approach can be applied reliably, as the second term on the rhs of Eq. (5) is already negligibly small.

IV. RESULTS AND DISCUSSION

A. Harmonic phonons

We first consider the pure Cr σ -phase. Having the same type of atoms on all crystallographic sites (CrCrCrCrCr), phonon results can better reveal features that depend only on the crystal structure.

Since the σ -phase contains 30 atoms, there are 3 acoustic modes and 87 optical modes, for a total of 90 normal vibrational modes. The resulting phonon dispersion curves are rather complex and present densely distributed optical branches above the acoustic ones, as shown in Fig. 2(a). No imaginary frequencies were found for this configuration. Vibrational frequencies range up to about 11 THz and there are no large gaps in the phonon DOS (Fig. 2(b)), although in the middle part of the spectrum there are several peaks emerging from the broad background. In the low-frequency part of the spectrum some soft modes from optical modes may be identified, although they are not very evident and overlap with the acoustic part of the spectrum. A similar behaviour was found for a toy system by Simdyankin *et al.*²¹

The phonon dispersion curves for the binary CrReCrRe configuration are shown in Fig. 3. With respect to the

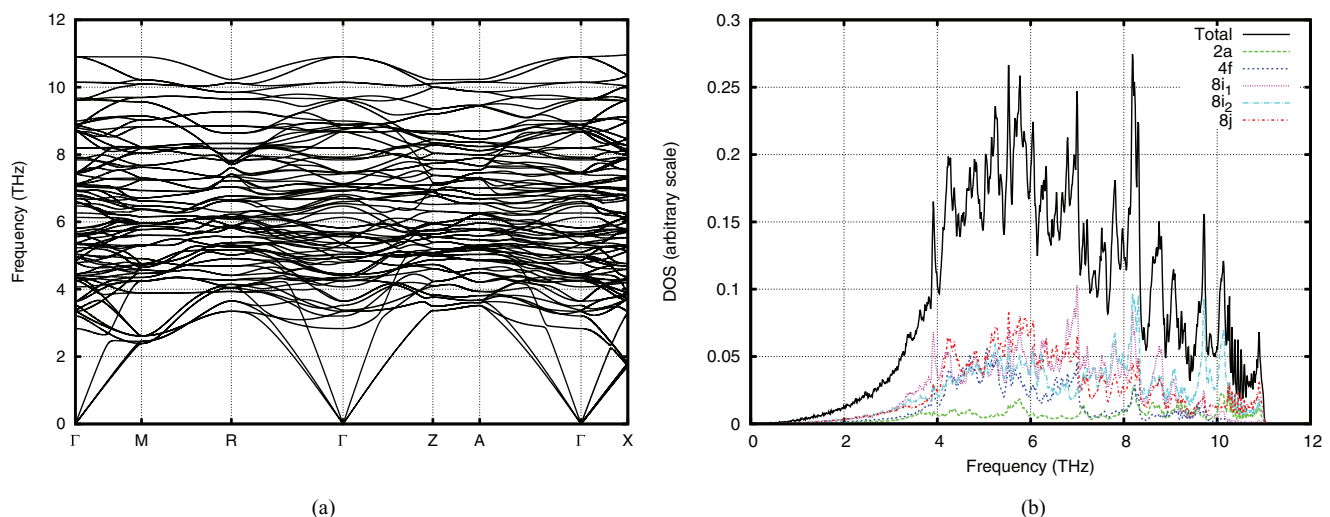


FIG. 2. Calculated phonon dispersion curves (a) and DOS (b) of the σ -phase for the CrCrCrCrCr configuration, where all crystallographic sites are occupied by Cr atoms. In (b) the projected DOS for the distinct crystallographic sites (2a, 4f, 8i₁, 8i₂, 8j) are also shown. The path was chosen along special points in the first Brillouin zone as in Ref. 21. Calculations are in the harmonic approximation.

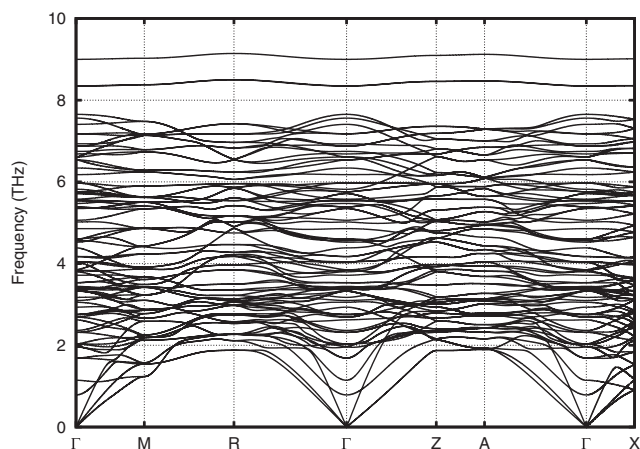


FIG. 3. Calculated phonon dispersion curves of the σ -phase for the selected binary configuration CrReCrReRe. The path was chosen along special points in the first Brillouin zone as in Ref. 21. Calculations are in the harmonic approximation.

pure Cr σ -phase (CrCrCrCrCr), Re atoms are present in the 4f, 8i₂ and 8j sites of the same crystal structure. Both chemical and structural effects can play a role in this case, i.e., effects which depend on the chemical properties of the atoms and on the features of the crystal structure, respectively. Overall, phonon frequencies are softened in comparison to the pure Cr σ -phase as a result of the presence of heavier Re atoms in some atomic sites. Some independent optical modes can be noted at high frequencies, in contrast to the pure Cr σ -phase. The presence of such independent modes was not found by Simdyankin *et al.*²¹ for a “pure” toy σ -phase model using empirical potentials but was found by Dubiel *et al.*¹⁵ for a binary Fe-Cr σ -phase using first principles. These independent modes are structurally related to the Wyckoff site 2a, mainly occupied by Cr atoms, as can be seen from the projected DOS reported in Fig. 4, coupled with sites 8i₂ and 8j. These latter sites are the nearest neighbours (NN) to the 2a site, with distances of 2.52 and 2.60 Å, respectively. The short distances result in high vibrational frequencies. However, as we have

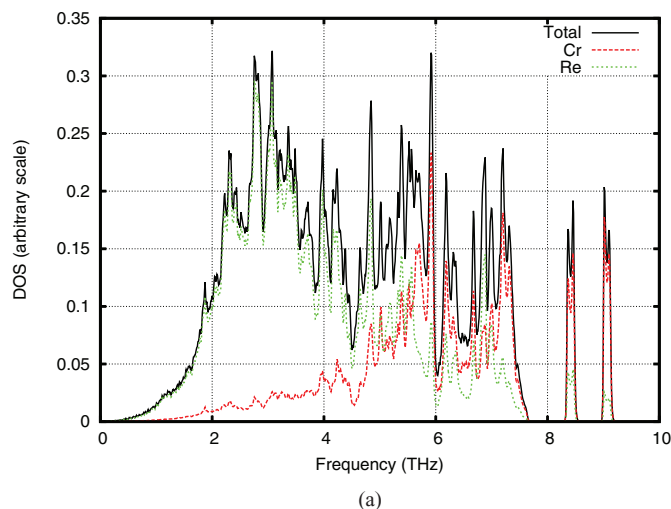


TABLE II. Thermodynamic properties for the binary CrReCrReRe configuration obtained using the direct force method in the harmonic approximation.

| T K | E_{harm} kJ/mol | $C_{v, \text{harm}}$ J/(mol K) | F_{harm} kJ/mol | S_{harm} J/(mol K) |
|------------|-----------------------------|-----------------------------------|-----------------------------|--------------------------------|
| CrReCrReRe | | | | |
| 300 | 7.862 | 23.72 | -2.888 | 35.832 |
| 600 | 15.158 | 24.63 | -16.435 | 52.655 |
| 1200 | 30.028 | 24.86 | -53.762 | 69.825 |
| 1800 | 44.962 | 24.91 | -98.888 | 79.916 |
| 2000 | 49.945 | 24.91 | -115.138 | 82.541 |

already remarked, no separate vibrational modes can be seen in the pure Cr σ -phase, although similarly the 2a site has as NN the 8i₂ and 8j sites. Thus, their appearance is related to chemical effects, when different types of atoms are present in the σ -structure, rather than structural effects.

According to their mass, in Fig. 4(a) vibrational modes related to Cr atoms dominate the high frequency part of the spectrum, while the opposite behaviour is observed for Re. In the low- and middle-frequency part of the DOS (Fig. 4(b)), vibrational modes related to the site 8i₁ (occupied by Re atoms) are prevalent at middle-high frequencies, while the modes related to the sites 4f and 8j (also occupied by Re atoms) have low frequencies. Cr atoms in the site 2a clearly vibrated at high frequency. These projected DOS appear rather different from those of the pure Cr σ -phase (Fig. 2(b)), where no clear predominance of any Wyckoff site was found in different frequency ranges of the density of states. From the above, it appears that there is a dominant mass effect on the DOS for the binary Cr-Re σ -phase. However, vibrational modes related to the site 8i₂ (occupied by Cr atoms) are spread over the entire frequency range, suggesting that structural effects also play a role.

In Table II, we report the harmonic Helmholtz energy (and other related quantities) as obtained from the computed phonon frequencies and Eq. (1).

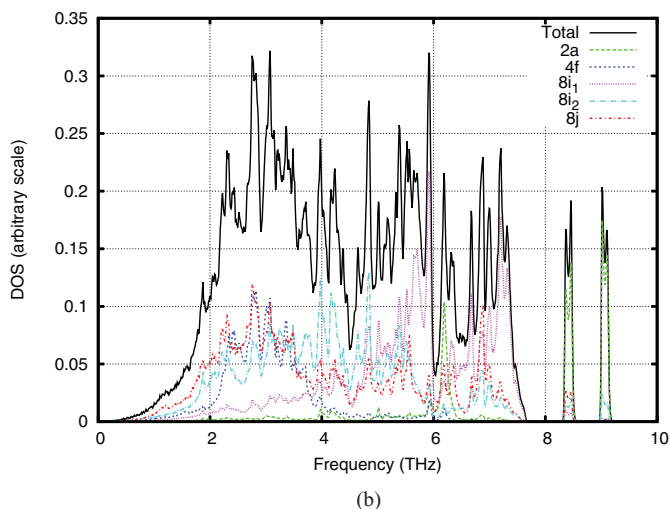


FIG. 4. Total and projected phonon DOS of the σ -phase for the selected binary configuration CrReCrReRe. (a) The projected DOS for atom type (Cr/Re). (b) The projected DOS for the distinct crystallographic sites (2a, 4f, 8i₁, 8i₂, 8j).

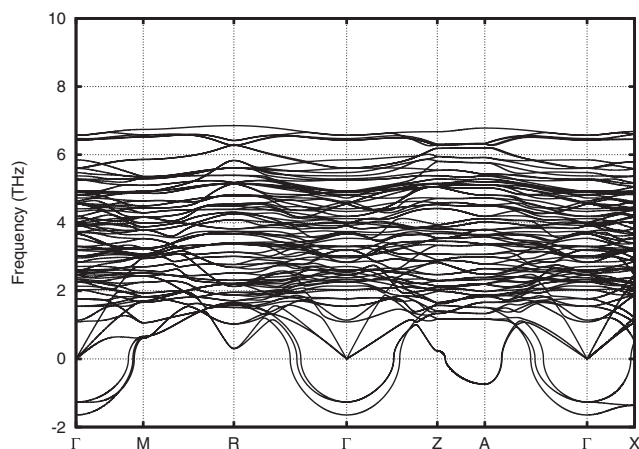


FIG. 5. Calculated phonon dispersion curves for the 90 vibrational modes of the σ -phase in the pure Re (ReReReReRe) configuration. The path was chosen along special points in the first Brillouin zone as in Ref. 21. Calculations are in the harmonic approximation.

B. Mechanical instability

When computing the phonon spectrum for the pure Re σ -phase, we found imaginary (negative) frequencies in the dispersion curves (Fig. 5), thus evidencing a mechanical instability in this structure at $T = 0$ K and $P = 0$ bar. As discussed in details in Ref. 39, the presence of imaginary frequencies means that a saddle point exists in the configurational space and the structure would spontaneously transform into a more stable one. As an example, one of the vibrational modes from which the imaginary frequencies arise is related to the vibration of the atoms in positions $8i_1$, $8i_2$, and $8j$ along the directions $(0,0,1)$, $(0,0,1)$, and $(1,1,0)$, respectively. Any small movement of these atoms along these directions will result in a structural change of the σ -phase structure. A pure Re σ -phase could not be the stable structure, being contrary to experimental evidence (Re is stable as an hcp structure). The present result shows that this structure is mechanically unstable and does not correspond to a local minimum in the configurational space.

In addition to the pure Re σ -phase, we found three more configurations to be mechanically unstable: CrReReReRe, ReCrReReRe, ReReCrReRe. In Fig. 6 we report our previously computed enthalpies of formation at 0 K for all binary Cr-Re configurations, showing by green line the mechanically unstable ones. It is evident that mechanical instability results in the Re-rich side. The additional unstable configurations occur when Cr substitutes Re in the $2a$, $4f$, and $8i_1$ sites of the pure Re σ -phase, but not when this happens in the $8i_2$ and $8j$ sublattices. The substitution of Cr in the first two low-multiplicity sites ($2a$ and $4f$) is clearly not sufficient to stabilize the structure with respect to the pure Re σ -phase. The composition of these two configurations is still very close to pure Re, with $X(\text{Re}) = 0.933$ and $X(\text{Re}) = 0.867$, respectively. More interesting is the mechanical instability originating from the substitution of Cr in the $8i_1$ site compared with in the $8i_2$ and $8j$ ones. In all three cases the final Re content is the same (0.733), but the mechanically unstable configuration ReReCrReRe has the higher enthalpy of formation at

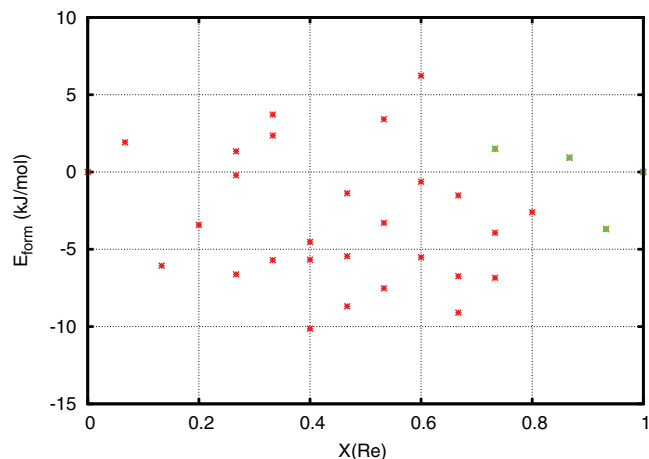


FIG. 6. Calculated enthalpies of formation at 0 K for all binary Cr-Re configurations of the σ -phase (adapted from Ref. 16). Reference states here the energies of pure Cr and Re in the σ -structure. The mechanically unstable configurations are shown by green line.

0 K (Fig. 6). Finally, we remark that the CrCrReReRe configuration, where Cr substitutes both $2a$ and $4f$ sites, has a higher Re content (0.8) but a lower enthalpy than the ReReCrReRe case and is mechanically stable.

C. Anharmonic effects

Little is known about the importance of anharmonic effects in the σ -phase. Based on their molecular dynamics simulations using an empirical potential for a toy one-component σ -phase, Simdyankin *et al.*²¹ concluded that the anharmonic contribution is negligible up to $0.2T_M$, where T_M is the melting (or solidus) temperature. Their conclusion is based on a qualitative analysis of the changes in the phonon spectrum obtained from molecular dynamics at high temperature.

The phonon DOS computed as Fourier transform of the normalized velocity autocorrelation function from our AIMD calculations are shown in Fig. 7 up to 1800 K ($\sim 0.7T_M$) for the binary CrReCrReRe σ -phase. Significant changes

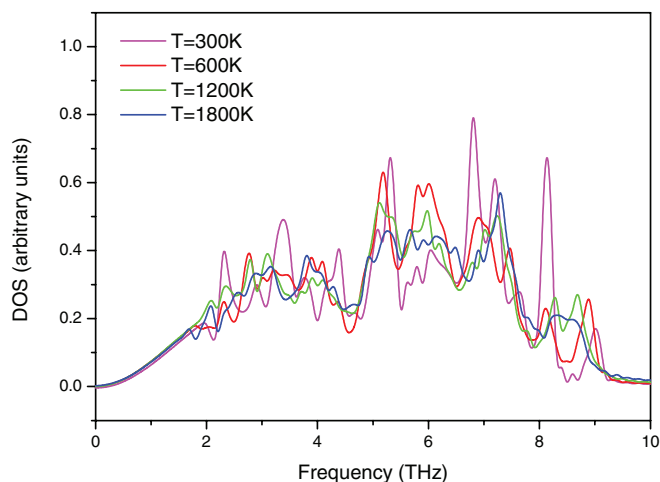


FIG. 7. Calculated phonon DOS obtained from the Fourier transform of the normalized velocity autocorrelation functions obtained using AIMD at different temperatures up to 1800 K for the binary CrReCrReRe σ -phase.

TABLE III. Anharmonic Helmholtz energy ($F_{\text{anh}} = F_{\text{vib}} - F_{\text{harm}}$) for the binary CrReCrReRe configuration in the σ -phase obtained using thermodynamic integration (TI) at different temperatures up to 2000 K. The last column is the statistical error in the evaluation of the average quantities.

| T K | F_{anh} kJ/mol | Statistical error kJ/mol |
|----------|----------------------------|-----------------------------|
| 500 | 0.10 | +− 0.03 |
| 1000 | 0.23 | +− 0.03 |
| 2000 | 0.54 | +− 0.07 |

occur in the high-frequency part of the spectrum increasing the temperature. For example, the two high-frequency peaks related to the 2a site are significantly modified at high temperature, evidencing a change in the local environment around this position. On the contrary, a limited effect can be noticed in the acoustic (Debye) part of the spectrum. Increasing the temperature, no softening of the acoustic modes is observed, what would be a typical sign of temperature-induced anharmonicity. This confirms the qualitative conclusion obtained by Simdyankin *et al.*²¹ and suggests low anharmonic effects in the binary CrReCrReRe σ -phase.

A quantitative evaluation of the anharmonic contribution to the Helmholtz energy based on TI is reported in Table III. Statistical errors in the values of the anharmonic contribution are also reported. The results confirm that anharmonic effects on thermodynamic quantities are negligible up to 2000 K ($\sim 0.8T_m$), with a maximum anharmonic Helmholtz energy of about 0.5 kJ/mol.

D. Thermodynamic properties of the harmonic σ -phase

We discuss in this section the thermodynamic properties of all binary Cr-Re (mechanically stable) configurations derived from the harmonic phonon frequencies. Figure 8 shows the calculated Helmholtz energies at different temperatures. Results for the enthalpies of formation, ZPE, Helmholtz

energies, entropies, and heat capacities are also reported in Table IV in the Appendix. Although we have remarked their limitations,²² we also show in this table the Einstein and Debye temperatures of all configurations for the sake of comparing their vibrational properties.

The ZPE (Fig. 8(a)) values range from a maximum value of 3.85 kJ/mol for the pure Cr σ -phase to 2.64 kJ/mol for the rightmost mechanically stable configuration (CrCrReReRe) in the Re-rich side of the plot. On the whole, differences in the ZPE among all configurations are small compared with their energies of formation at 0 K (Fig. 6) and thus have limited consequences on their relative stability. The vibrational Helmholtz energies have more dramatic effects, depending on the temperature. As shown in Fig. 8(b), the differences in Helmholtz energies among all configurations at 2000 K are significantly higher than ZPE and comparable with the energies of formation at 0 K. To better evaluate this effect, we show in Fig. 9 the sum of the enthalpies of formation and harmonic Helmholtz energies of all configurations at two different temperatures (2000 and 3000 K). It is clear that the vibrational contribution significantly alters the relative stability of the configurations with respect to the enthalpy of formation at 0 K (Fig. 6), reducing their differences in energy. Taking as an example the configurations at $X(\text{Re}) = 0.467$ (ReReCrCrRe, ReReCrReCr, ReReReCrCr), the maximum difference in energy at 0 K is 7.32 kJ/mol, but it reduces to 3.24 kJ/mol at 2000 K and to 1.21 kJ/mol at 3000 K. This behaviour strongly favours the disordering of the σ -phase on increasing the temperature. A Bragg-Williams approach neglecting vibrational contributions to the Helmholtz energy can thus lead to a significant underestimation of disordering phenomena at high temperature. Finally, taking as another example the configurations at $X(\text{Re}) = 0.667$ (CrReReReCr, CrReReCrRe, CrReCrReRe), Fig. 10 shows that the most stable configuration at 0 K is CrReReCrRe, whereas on increasing the temperature the most stable configuration becomes CrReCrReRe because of the different vibrational contributions to the Helmholtz energy. Similar behaviour is observed at different compositions (not shown).

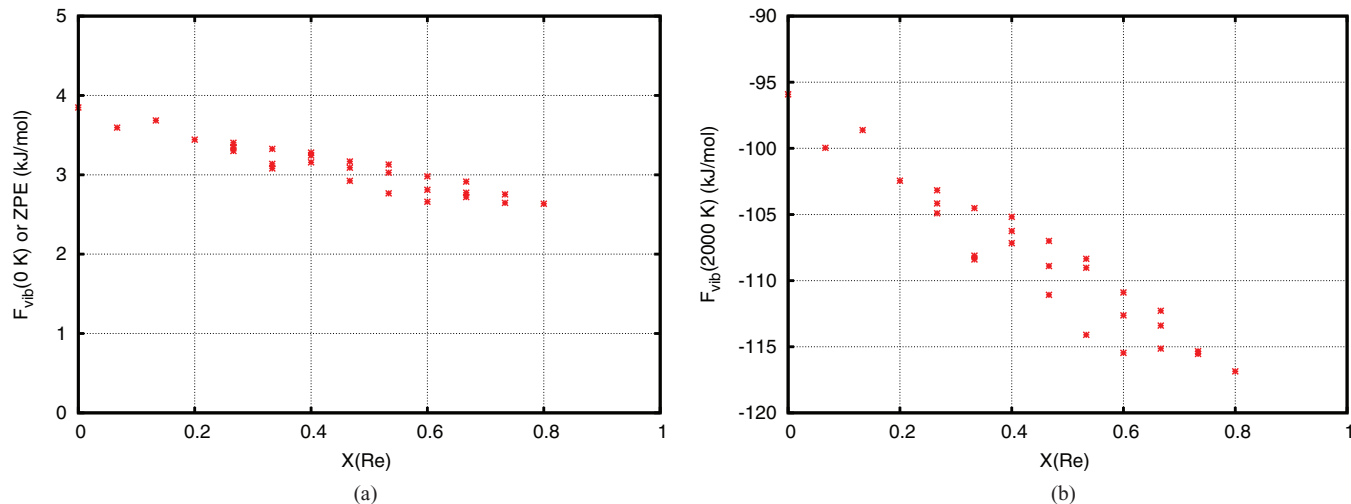


FIG. 8. Calculated harmonic Helmholtz energy at 0 K (a), 2000 K (b), and 3000 K (c) of all binary (mechanically stable) Cr-Re configurations of the σ -phase.

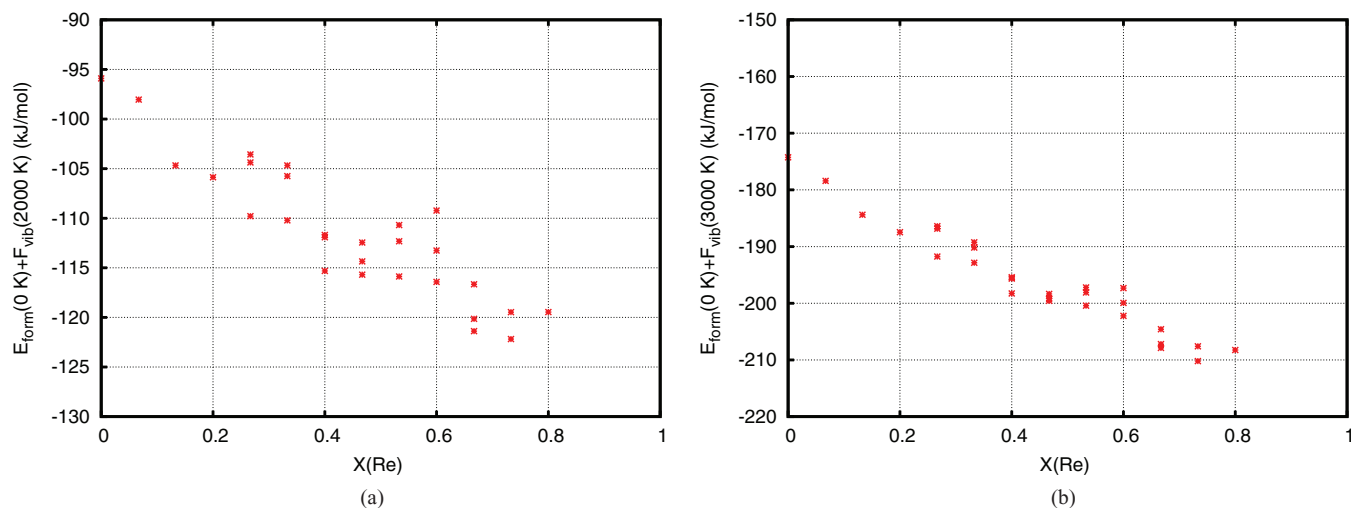


FIG. 9. Calculated enthalpies of formation plus harmonic Helmholtz energy at 2000 K (a) and 3000 K (b) of all binary (mechanically stable) Cr-Re configurations of the σ -phase.

V. CONCLUSION

In this work, we have evaluated harmonic and anharmonic vibrational effects in the Cr-Re σ -phase. In the harmonic approximation, we did not find clear structural effects in the phonon DOS when examining the pure Cr σ -phase, while the structure was found to be mechanically unstable when all sites are occupied by Re atoms. In the binary Cr-ReCrReRe σ -phase, we found independent vibrational modes arising from the difference between Cr and Re atomic masses. Mass effects appear to be dominant with respect to structural effects in the binary case, although the latter also play a role.

AIMD simulations at high temperature show remarkable changes in the high-frequency part of the phonon spectrum, for example, evidencing a change in the local environment around the site 2a. By contrast, minor changes occur in the low-frequency (Debye) part of the spectrum, suggesting low anharmonic effects on thermodynamic functions. This was quantitatively confirmed by using thermodynamic integration.

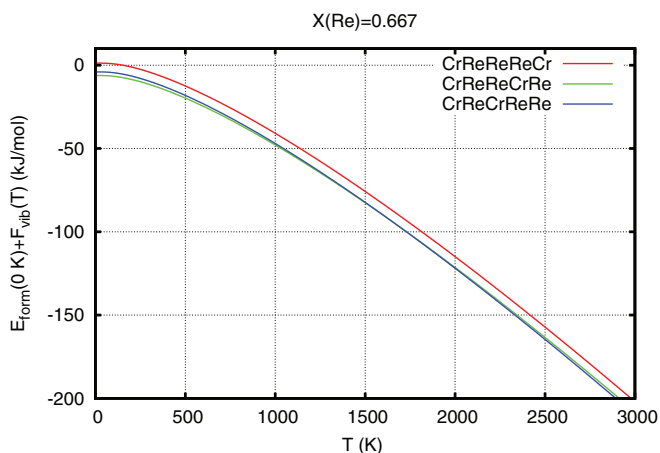


FIG. 10. Calculated enthalpies of formation plus harmonic Helmholtz energy as a function of temperature for the 3 configurations at $X(\text{Re}) = 0.667$.

A negligible anharmonic contribution to the Helmholtz energy was found up to 2000 K ($\sim 0.8T_m$) in the binary CrReCrReRe σ -phase. The present results on the anharmonicity need to be extended to other TCP phases to verify if the present findings are more general.

The vibrational contribution significantly alters the relative stability of the configurations with respect to the enthalpy of formation at 0 K. Changes in the most stable configuration for a given composition are observed because of the difference in the harmonic Helmholtz energy as a function of temperature. The vibrational contribution strongly reduces the differences in energy among all configurations thus favouring the disordering of the σ -phase on increasing the temperature. As a consequence, a Bragg-Williams approach neglecting vibrational contributions to the Helmholtz energy is expected to fail in correctly describing the full disordering behaviour.

ACKNOWLEDGMENTS

M.P. and S.G.F. acknowledge funding from ICAMS which is supported by ThyssenKrupp AG, Bayer Material Science AG, Salzgitter Mannesmann Forschung GmbH, Robert Bosch GmbH, Benteler Stahl/Rohr GmbH, Bayer Technology Services GmbH, the state of North-Rhine Westphalia, the European Commission in the framework of the ERDF and the Deutsche Forschungsgemeinschaft (DFG) through Project No. C6 of SFB/TR 103. Part of the molecular dynamics simulations were performed on the U.K. National system HECToR. M.P. thanks V. A. Yardley for proof reading the paper.

APPENDIX: HARMONIC RESULTS

See Table IV.

TABLE IV. Thermodynamic properties of all binary Cr-Re configurations of the σ -phase. For mechanically unstable configurations, only the enthalpy of formation at 0 K is reported. Einstein and Debye temperatures were computed by fitting the harmonic heat capacity from 0 to 3000 K.

| Conf. | X(Re) | $E_{\text{form}}(0 \text{ K})$ kJ/mol | ZPE kJ/mol | $F_{\text{harm}}(2000 \text{ K})$ kJ/mol | $S_{\text{harm}}(2000 \text{ K})$ J/mol/K | $C_{\text{harm}}(2000 \text{ K})$ J/mol/K | θ_E K | θ_D K |
|------------|-------|--|---------------|---|--|--|-----------------|-----------------|
| CrCrCrCrCr | 0 | 0 | 3.85 | -95.91 | 72.95 | 24.89 | 301.7 | 407.8 |
| CrCrCrCrRe | 0.267 | -0.21 | 3.35 | -104.17 | 77.07 | 24.9 | 259.7 | 351.4 |
| CrCrCrReCr | 0.267 | 1.34 | 3.30 | -104.91 | 77.44 | 24.9 | 256.7 | 347.2 |
| CrCrCrReRe | 0.533 | 3.41 | 2.77 | -114.1 | 82.02 | 24.91 | 214 | 289.6 |
| CrCrReCrCr | 0.267 | -6.62 | 3.40 | -103.17 | 76.57 | 24.9 | 264.6 | 357.9 |
| CrCrReCrRe | 0.533 | -7.52 | 3.13 | -108.35 | 79.16 | 24.91 | 240.9 | 326.1 |
| CrCrReReCr | 0.533 | -3.29 | 3.03 | -109.03 | 79.5 | 24.91 | 235 | 317.9 |
| CrCrReReRe | 0.8 | -2.6 | 2.64 | -116.86 | 83.4 | 24.92 | 202.7 | 274.4 |
| CrReCrCrCr | 0.133 | -6.06 | 3.68 | -98.62 | 74.3 | 24.89 | 288.1 | 389.5 |
| CrReCrCrRe | 0.4 | -5.67 | 3.24 | -106.25 | 78.11 | 24.9 | 250.8 | 339.4 |
| CrReCrReCr | 0.4 | -4.52 | 3.16 | -107.17 | 78.57 | 24.91 | 245.4 | 331.9 |
| CrReCrReRe | 0.667 | -1.52 | 2.72 | -115.14 | 82.54 | 24.92 | 209.7 | 283.8 |
| CrReReCrCr | 0.4 | -10.13 | 3.28 | -105.18 | 77.57 | 24.9 | 254.8 | 344.7 |
| CrReReCrRe | 0.667 | -9.1 | 2.91 | -112.28 | 81.12 | 24.91 | 223.5 | 302.6 |
| CrReReReCr | 0.667 | -6.74 | 2.77 | -113.4 | 81.67 | 24.91 | 215.1 | 291 |
| CrReReReRe | 0.933 | -3.69 | ... | ... | ... | ... | ... | ... |
| ReCrCrCrCr | 0.067 | 1.92 | 3.59 | -99.96 | 74.97 | 24.9 | 280.7 | 379.5 |
| ReCrCrCrRe | 0.333 | 2.36 | 3.14 | -108.11 | 79.04 | 24.91 | 242.5 | 328.2 |
| ReCrCrReCr | 0.333 | 3.72 | 3.08 | -108.4 | 79.18 | 24.91 | 239.8 | 324.4 |
| ReCrCrReRe | 0.6 | 6.23 | 2.66 | -115.46 | 82.7 | 24.92 | 207.2 | 280.2 |
| ReCrReCrCr | 0.333 | -5.7 | 3.33 | -104.52 | 77.24 | 24.9 | 258.2 | 349.2 |
| ReCrReCrRe | 0.6 | -5.52 | 2.98 | -110.9 | 80.43 | 24.91 | 228.9 | 310 |
| ReCrReReCr | 0.6 | -0.63 | 2.81 | -112.63 | 81.29 | 24.91 | 218.8 | 296 |
| ReCrReReRe | 0.867 | 0.93 | ... | ... | ... | ... | ... | ... |
| ReReCrCrCr | 0.2 | -3.42 | 3.44 | -102.45 | 76.21 | 24.9 | 268.3 | 362.9 |
| ReReCrCrRe | 0.467 | -5.45 | 3.09 | -108.9 | 79.43 | 24.91 | 238.3 | 322.6 |
| ReReCrReCr | 0.467 | -1.37 | 2.92 | -111.08 | 80.51 | 24.91 | 227.3 | 307.4 |
| ReReCrReRe | 0.733 | 1.5 | ... | ... | ... | ... | ... | ... |
| ReReReCrCr | 0.467 | -8.69 | 3.17 | -107 | 78.48 | 24.91 | 245.7 | 332.4 |
| ReReReCrRe | 0.733 | -6.84 | 2.75 | -115.34 | 82.64 | 24.91 | 210.4 | 285 |
| ReReReReCr | 0.733 | -3.93 | 2.65 | -115.54 | 82.74 | 24.92 | 206 | 278.6 |
| ReReReReRe | 1 | 0 | ... | ... | ... | ... | ... | ... |

- ¹C. M. Rae and R. C. Reed, *Acta Mater.* **49**, 4113 (2001).
²M. Dzugutov, *Phys. Rev. A* **46**, R2984(R) (1992).
³J. Roth and F. Gálher, *Eur. Phys. J. B* **6**, 425 (1998).
⁴J.-M. Joubert, *Prog. Mater. Sci.* **53**, 528 (2008).
⁵J.-M. Joubert and M. Phejar, *Prog. Mater. Sci.* **54**, 945 (2009).
⁶M. Sluiter, K. Esfarjani, and Y. Kawazoe, *Phys. Rev. Lett.* **75**, 3142 (1995).
⁷C. Berne, M. Sluiter, Y. Kawazoe, T. Hansen, and A. Pasturel, *Phys. Rev. B* **64**, 144103 (2001).
⁸M. H. F. Sluiter, A. Pasturel, and Y. Kawazoe, *Prediction of Site Preference and Phase Stability of Transition Metal Based Frank-Kasper Phases in the Science of Complex Alloy Phases* (TMS, Warrendale, PA, 2005).
⁹P. A. Korzhavyi, B. Sundman, M. Selleby, and B. Johansson, *Mater. Res. Soc. Symp. Proc.* **842**, 517 (2005).
¹⁰O. Grånas, P. A. Korzhavyi, A. E. Kissavos, and I. A. Abrikosov, *CALPHAD* **32**, 171 (2008).
¹¹M. Sluiter and A. Pasturel, *Phys. Rev. B* **80**, 134122 (2009).
¹²J. Pavlů, J. Vřešťál and M. Šob, *Intermetallics* **18**, 212 (2010).
¹³J.-C. Crivello, M. Palumbo, T. Abe, and J.-M. Joubert, *CALPHAD* **34**, 487 (2010).
¹⁴J.-C. Crivello and J.-M. Joubert, *J. Phys. Condens. Matter.* **22**, 035402 (2010).
¹⁵S. M. Dubiel, J. Cieslak, W. Sturhahn, M. Sternik, P. Piekarz, S. Stankov, and K. Parlinski, *Phys. Rev. Lett.* **104**, 155503 (2010).
¹⁶M. Palumbo, T. Abe, S. G. Fries, and A. Pasturel, *Phys. Rev. B* **83**, 144109 (2011).
¹⁷E. Kabliman, P. Blaha, K. Schwarz, A. V. Ruban, and B. Johansson, *Phys. Rev. B* **83**, 092201 (2011).
¹⁸K. Yaqoob, J.-C. Crivello, and J.-M. Joubert, *Inorg. Chem.* **51**, 3071 (2012).
¹⁹J. Häfner, *From Hamiltonians to Phase Diagrams* (Springer-Verlag, Berlin, 1987).
²⁰W. Kress, *Phonon Dispersion Curves, One-Phonon Densities of States and Impurity Vibrations of Metallic Systems* (Fachinformationzentrum Karlsruhe, Karlsruhe, 1987).
²¹S. I. Simdyankin, S. N. Taraskin, M. Dzugutov, and S. R. Elliott, *Phys. Rev. B* **62**, 3223 (2000).
²²M. Palumbo, T. Abe, J.-C. Crivello, A. Breidi, J.-M. Joubert, S. G. Fries, T. Hammerschmidt, and R. Drautz, *Comput. Mater. Sci.* **81**, 433 (2014).
²³M. Palumbo, B. Burton, A. Costa e Silva, B. Fultz, B. Grabowski, G. Grimvall, B. Hallstedt, O. Hellman, B. Lindahl, A. Schneider, P. E. A. Turchi, and W. Xiong, *Phys. Status Solidi* **251**, 14 (2014).
²⁴B. Fultz, *Prog. Mater. Sci.* **55**(4), 247 (2010).
²⁵A. van de Walle and G. Ceder, *Rev. Mod. Phys.* **74**, 11 (2002).
²⁶M. Palumbo, T. Abe, C. Kocer, H. Murakami, and H. Onodera, *CALPHAD* **34**, 495 (2010).
²⁷J. S. Kasper, *Atomic and Magnetic Ordering in Transition Metal Structure in Theory of Alloy Phases* (ASM, Cleveland, OH, 1956).
²⁸J. S. Kasper and R. M. Waterstrat, *Acta Crystallogr.* **9**, 289 (1956).
²⁹G. Kresse and J. Hafner, *Phys. Rev. B* **47**, 558 (1993).
³⁰G. Kresse and J. Furthmüller, *Comput. Mater. Sci.* **6**, 15 (1996).
³¹G. Kresse and J. Furthmüller, *Phys. Rev. B* **54**, 11169 (1996).
³²J. P. Perdew, *Electronic Structures of Solids* (Akademie Verlag, Berlin, 1991).

- ³³H. J. Monkhorst and J. D. Pack, *Phys. Rev. B* **13**, 5188 (1976).
- ³⁴D. Alfè, *Comput. Phys. Commun.* **180**, 2622 (2009).
- ³⁵D. Alfè, *Comput. Phys. Commun.* **118**, 31 (1999).
- ³⁶M. Sampoli, P. Benassi, R. Dell'Anna, V. Mazzacurati, and G. Ruocco, *Philos. Mag. B* **77**, 473 (1998).
- ³⁷J. M. Dickey and A. Paskin, *Phys. Rev.* **188**, 1407 (1969).
- ³⁸D. Alfè, G. D. Price, and M. J. Gillan, *Phys. Rev. B* **64**, 045123 (2001).
- ³⁹G. Grimvall, B. Magyar-Köpe, V. Ozoliņš, and K. A. Persson, *Rev. Mod. Phys.* **84**, 945 (2012).